Structural and in vitro study of the β-Barrel Assembly Machine in Gram negative bacteria

Hans Bergal

Committee Members
Marcelo Sousa, Ph.D: Department of Chemistry and Biochemistry
Joseph Falke Ph.D: Department of Chemistry and Biochemistry
Jennifer Martin, Ph,D: Department of Molecular, Cellular, and Developmental Biology

Undergraduate Thesis
Spring 2017

Research Advisor: Marcelo Sousa, Ph.D

University of Colorado at Boulder
Department of Chemistry and Biochemistry

Table of Contents

Abstract

The β-Barrel assembly machine (BAM) catalyzes the folding and insertion of outer membrane proteins (OMP) in gram-negative bacteria. The protein complex is essential for cell survival due to its critical role in folding the vast number of outer membrane proteins. However, the mechanism by which BAM recognizes, folds, and inserts OMPs is still poorly understood. Of the five subunits in the BAM complex, only BamA and BamD are essential for cell viability. Here, a crystal structure of a BamA-BamD fusion protein from Rhodothermus Marinus is presented and shown to capture the native interaction. I also demonstrate a proof of concept in vitro OMP folding model based on an in vitro transcription translation system which could be used to probe the BAM folding mechanism. The in vitro assay could be further developed to more accurately replicate in vivo folding conditions compared to existing in vitro models.

Introduction

Gram-negative bacteria are a general class of bacteria which include common bacterial strains like E. coli, Salmonella and Yersinia. One of the defining characteristics of gram-negative bacteria is a double membrane. The inner membrane is a phospholipid bilayer which separates the cytosol from the intermembrane space, called the periplasm. The outer membrane is an asymmetric bilayer with lipopolysaccharide (LPS) facing outward and phospholipids facing inward. The outer membrane serves as a selective barrier, allowing uptake of nutrients and release of waste while protecting the cell from toxins. All molecules must pass through the outer membrane either by diffusing through the membrane or passing through protein porins to enter the cell (Nikaido, 2003). Understanding membrane dynamics could have implications for antibiotic uptake and targeting, making the outer membrane an interesting area of research.

The outer membrane contains many membrane proteins involved in a wide variety vital functions such as membrane assembly, nutrient uptake and effector secretion. Almost all outer membrane proteins contain a β-barrel integral membrane domain. This β-barrel membrane domain is composed of an even number of anti-parallel β-strands which curve around to form a cylinder. In some cases, the β-barrel serves as a simple porin, like OmpF which transports small ions across the outer membrane. Other β-barrels are part bacterial adhesion to eukaryotic cells like OmpX or help assemble the LPS like LptD (Koebnik et al., 2000; Hagan et al., 2011).

Outer membrane proteins are synthesized in the cytosol and are tagged for transport across the inner membrane with a N-terminal signal sequence. After synthesis, they are post-translationally transported across the inner membrane to the periplasm through the Sec translocon and the signal sequence is cleaved. There are several periplasmic chaperones, SurA, Skp, and DegP, which bind and prevent aggregation of OMPs as they move across the periplasm (Lyu and Zhao, 2015). The OMPs are then folded and inserted into the outer membrane by the

β-barrel Assembly Machine (BAM) complex. The BAM complex is required to catalyze insertion β-barrels however the exact mechanism of β-barrel recognition, folding, and insertion by the BAM complex into the outer membrane is still poorly understood (Plummer and Flemming, 2016).

In E. coli, the BAM complex is composed of five subunits. BamA is the central component with a β-barrel membrane domain and five soluble Polypeptide Translocation Associated (POTRA) domains which extend into the periplasm. The four other subunits, BamB, BamC, BamD and BamE, are peripheral membrane proteins anchored to the outer membrane through a N-terminal cysteine. The lipoproteins are first attached to a diacylglycerol on phosphatidylglycerol lipids and another acyl group is attached to amine group on the cysteine to further anchor the lipoprotein in the membrane (Wolfram, 2014) . Deletion of BamB, BamC and BamE lead to growth defects and increased antibiotic susceptibility due to membrane defects (Onufryk et al, 2005). BamA and BamD are both essential for survival in E. coli and are highly conserved across all gram-negative bacteria, suggesting the fundamental importance of both subunits for OMP folding (Maliniverni et al., 2006).

The crystal structures of all individual BAM subunits had been previously solved (Albrecht and Zeth, 2011; Endo et al., 2011; Heuck et al., 2011; Jansen et al., 2012; Kim and Paetzel, 2011; Knowles et al., 2011; Noinaj et al., 2011, 2013; Sandoval et al., 2011;Warner et al., 2011). Biochemical data suggested BamCDE forms a subcomplex that interacts with BamA, with BamB binding to BamA independently (Kim et al., 2007). Consistent with this model, Crystal structures capturing BamA-B fragments as well as BamC-D have been solved, (Jansen et al., 2015; Kim et al., 2011). However, the BamA-BamD interface was previously unknown.

Here, we report the crystal structure of a BamA-BamD fusion protein capturing the native interface between the two subunits.

Since the OMP folding pathway is essential, manipulation of the BAM complex in vivo gives limited information on the activity of BAM. Mutations that effect BAM activity might still be functional enough that cell growth or membrane permeability is not measurably altered. On the other hand, when a mutation inhibits BAM activity to below a required threshold for cell growth, the cells are non-viable and die. It is impossible to tell if one lethal mutation had a stronger effect than another lethal mutation since the only observable is cell death. This limits the quantitative biochemical characterization of in vivo BAM activity because the primary read out is cell viability. For example, opening and closing of the β-barrel is thought to be important for OMP insertion. In fact, locking the barrel with cysteines leads to cell death (Noniaj et al., 2015). However, since the cell dies the direct impact on folding rates cannot be determined. Having an in vitro model where BAM activity could be directly measured would allow direct quantification of effects of BAM mutants which could help uncover the folding mechanism. In vitro models have been previously developed but rely on artificially high concentrations of protein denatured in urea (Hagan et al., 2010; Roman-Hernandez et al.,2014). We discuss the development of a new in vitro model which uses an in vitro transcription translation system to more accurately replicate in vivo conditions.

Results and Discussion

Crystal Structure of BamA-BamD fusion

The central component of the BAM complex is BamA, which has a β-barrel membrane domain and 5 periplasmic POTRA domains. Due to the membrane domain of BAM, structural characterization of the full complex is difficult. By solving the structure in smaller fragments, a

full model could be built without having to purify and crystallize the entire complex. The general strategy was to only use a soluble fragment of BamA and co-crystallize it with BamD to give a structure of the interface between the two subunits.

Previous biochemical data suggested that BamD interacted with POTRA5 of BamA, making POTRA5 a target for co-crystallization with BamD. BamA mutants with POTRA domain deletions had been previously tested for their ability to pull down the BamCDE subcomplex. BamA with deletions in POTRA1-4 were still able to copurify with BamCDE proteins however POTRA5 deletion lost binding to BamCDE (Kim et al., 2007). This suggested that POTRA5 was the primary domain meditating the BamA-BamCDE interaction.

Further evidence suggested that BamD was making an essential contact point with POTRA5. A point mutation was identified on POTRA 5 of BamA, BamA E373K, which gave a lethal cell phenotype. This phenotype was found to be rescued by a compensatory mutation on BamD, BamD R197L. This suggests a favorable charge interaction between the glutamic acid on BamA and the arginine on BamD was initially disrupted, which supports that the POTRA5 domain of BamA was in direct contact with BamD (Ricci et al., 2012). Based on this data, several constructs were designed containing fragments of BamA POTRA5 and BamD, eliminating the need of purifying and crystallizing the transmembrane domain.

The major obstacle in determining the BamA-BamD interface was obtaining crystals with the subunits interacting with their native interface. It was predicted that if BamA and BamD crystallized together, the two subunits would adopt the native interface within the crystal structure. However, when crystallization was attempted with copurifed BamA and BamD, no were found which conditions yielded diffractable conditions. To increase the chances of BamA and BamD forming a crystallizable complex, the soluble portion of BamA and BamD were fused

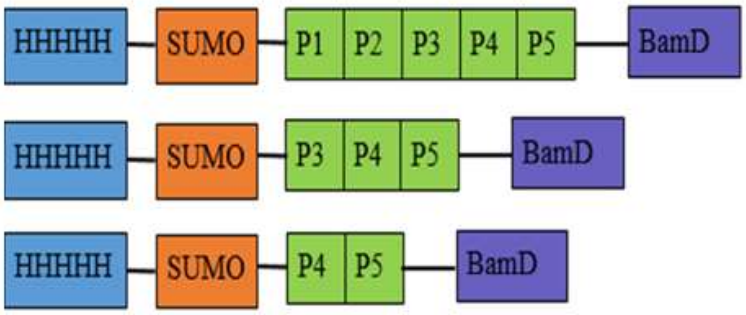

Figure 1. Three constructs tested for expression and purification. Full Length construct with His-tag, cleavable SUMO tag, Rhodothermus BamA POTRA1-5, fusion linker and Rhodthermus BamD. Two truncated constructs with BamA POTRA3-5 and POTRA4-5.

together with a flexible linker. By linking the two subunits together, there would be a high local concentration of BamA and BamD near each other which would promote crystallization of the subcomplex. Furthermore, the fusion linker would ensure that BamA and BamD would purify in the correct 1:1 stoichiometric ratio, further increasing the chances that the two subunits would crystallize together. In addition, homologous BAM proteins from the thermophile Rhodothermus Marinus were used as proteins from thermophilic organisms often yield better ordered crystals (McPherson and Cudney, 2014).

In order to capture the native BamA-BamD interface using the fusion approach, strategic placement and length of the linker was essential. Based on the previously solved crystal structure of BamA, the C terminus of POTRA5 is close to the outer membrane. Since BamD is anchored to the outer membrane by its N terminus, it was reasoned that connecting the C terminus of POTRA5 to the N terminus of BamD could allow the BamA and BamD to bind with their native interface. A 22-amino acid glycine-serine linker connected the C terminus of POTRA5 and the N terminus of BamD. The linker has an approximate length of 75 Å, allowing BamD to sample most conformations while keeping the two subunits near. A similar fusion strategy had been previously used to successfully solve the structure of BamA-BamB (Jansen et al., 2015).

Three constructs were designed and tested for purification and crystallization (figure 1). The full-length construct contains POTRA1-5 and BamD connected with the linker. BamA

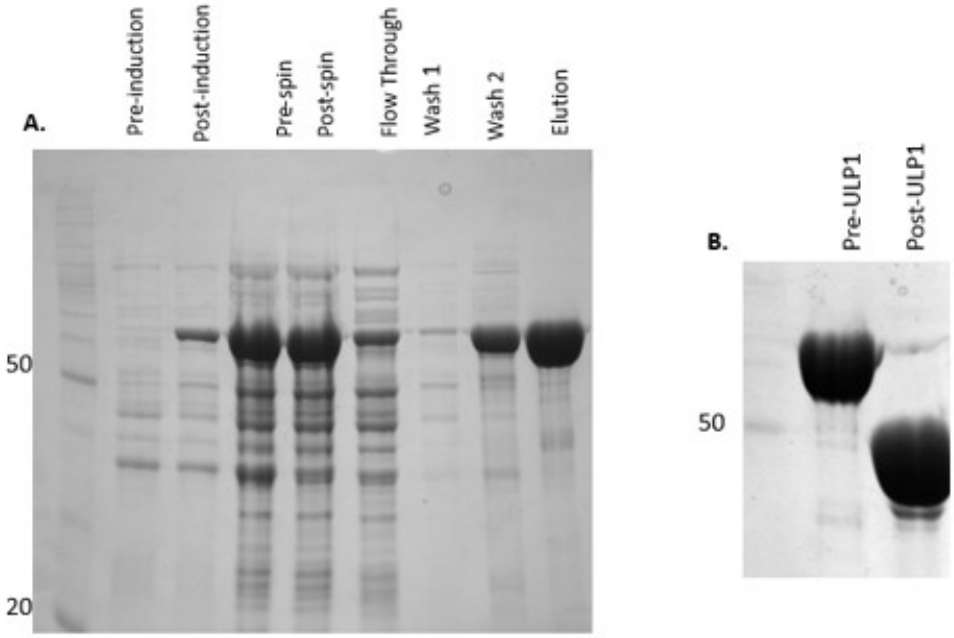

Figure 2. Purification of Fusion Protein
Purification samples for POTRA-4-5 Nickel-NTA purification (A). Expected protein size is 65 kDa. Pre-induction: whole cells before IPTG induction. Post-induction: whol cells after overnight incubation with IPTG. Cells were lysed (pre-spin) and centrifuged to remove unlysed cells (post-spin). Lysate was poured over Nickel-NTA column and Flow through collected. Washed first with 25 mM Tris pH 8.0, 150 mM NaCl (wash 1), then with the same buffer with 20 mM imidazole (wash 2). Eluted in buffer with 200 mM imidazole. B. Before and after ULP-1 cleavage of SUMO tag. Weight shift indicates successful cleavage. Sample was subsequently loaded onto size exclusion column. BamA-D protein is predicted to be 50 kDa. without tag.

contains a flexible hinge between POTRA2 and 3, which could interfere with crystallization. Since BamD most likely interacted with POTRA5, two truncated constructs with POTRA3-5 and POTRA4-5 were also tested which omit the flexible hinge while retaining the BamA POTRA domains predicted to interact with BamD. All three constructs have a His-tag for purification and a SUMO tag for subsequent cleavage.

The three constructs were introduced to cells and initially tested for favorable purification conditions. The BamA POTRA 4-5 BamD construct expressed well and was purified through affinity chromatography with a Ni-NTA column. SDS-PAGE analysis of the samples taken from different steps of Ni-NTA column purification indicate that the construct was successful purified (figure 2A). A clear band appears in the whole cell lysate after induction with IPTG at the

predicted molecular weight 65 kDa which is not present in the whole cell lysate before induction. The band is significantly enriched in the elution sample from the nickel column which indicates that the BamA POTRA 4-5 BamD construct was expressed after induction and pulled down with the nickel column. Both BamA POTRA 3-5 BamD and BamA POTRA 1-5 BamD constructs were expressed but would aggregate upon further purification (data not shown). Changes in bacterial growth media, IPTG induction concentration, induction incubation time, presence of detergents, buffer pH, salt concentration and oxidizing agents were all tested to optimize BamA POTRA 3-5 BamD and BamA POTRA 1-5 BamD purification. However suitable expression conditions could only be identified for the BamA POTRA4-5 BamD construct.

To prepare the POTRA4-5 BamD for crystallization, the cleavable tag was removed and further purified with size exclusion chromatography. After the BamA POTRA4-5 BamD construct was initially enriched with affinity chromatography, the SUMO tag was cleaved with Ubiquitin-like-specific protease 1 (ULP1), leaving only BamA-BamD sequence. The weight shift from 65 kDa before to ULP1 treatment to 50 kDa after treatment indicates that the tag was successfully cleaved (figure 2B). This was an important step to ensure that the purification tag did not interfere with either the crystallization process or native structure of BamA or BamD. The BamA-BamD protein was separated from the cleavable tag along with other proteins impurities still present using size exclusion chromatography. Fractions containing the fusion construct were identified with an SDS PAGE gel, pooled together and concentrated.

The next step was to find conditions which would promote formation of crystals of the purified BamA-BamD protein to use to collect x-ray diffraction data. The BamA-BamD fusion protein was initially screened for crystallization conditions using the sitting drop method and several commercial screens (see methods). The commercial screens have large arrays of different

salts are varying concentrations, other additives like polyethylene glycol (PEG) or Tris, and pH

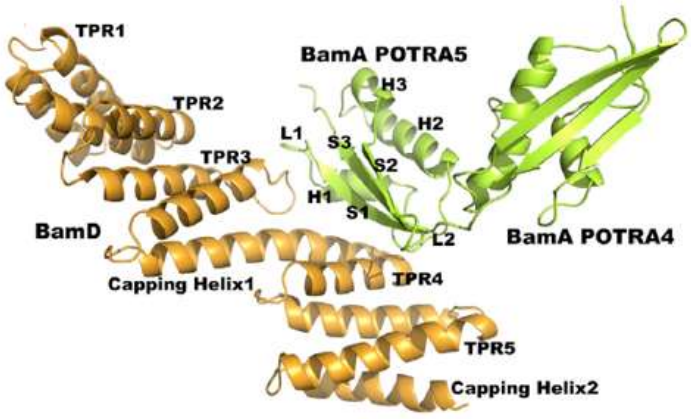

Figure 3. Structure of BamA POTRA4-5 and BamD Cartoon representation of the crystal structure of Rhodothermus BamA POTRA4-5 (Yellow) and BamD (orange). BamD interacts only with POTRA5 and does not have contact with POTRA 4. TPR domains 3 and 4 of BamD form the major contact points with BamA. For BamA, POTRA5 α-1 and β-1 strands along with the connecting loops L1 and L2 form the interface with BamD.

conditions which affect protein solubility and attempt to slowly precipitate out the protein to form ordered crystals. Using commercial screens, numerous screening conditions yielded small needle like crystals but were not suitable for x- ray diffraction data collection. Initial conditions which yielded crystals were optimized using hanging drop trays set up by hand. Final conditions of 10% PEG 3000, 15% Isopropyl alcohol, 0.1M HEPES pH 5.6 yielded thin (<1 mm) plates around 0.5x 1 cm. Suitable crystals were harvested, transferred to a cryoprotectant and frozen in liquid nitrogen. Crystals were shipped to Advanced Light Source at the Lawrence Berkeley National Laboratory for data collection. I collected diffraction data to 2.0 Å resolution and the data was used by my advisor to determine the structure by molecular replacement (Figure 3).

The solved structure of the Rhodothermus BamA POTRA4-5 BamD is shown in figure 3. BamD, shown in orange, is composed of five tetratricopeptide repeats (TPR). TPR motifs contain are two α-helices connected with a loop region, with TPR 1 at the N-terminus. BamA POTRA domains 4-5 are shown in yellow. POTRA domains have a β1-α1- α2- β2- β3 folding motif which is seen in POTRA4 (Gatzeva-Topalova et al., 2008; Kim et al., 2007). However, the POTRA5 has a small, extra α-helix (α3) between α2 and β2 secondary structures. This extra α-

helix is present in the Rhodothermus Bam structure but is not in previous E. coli BamA structures (Gatzeva-Topalova et al., 2010). The BamA-BamD interface occurs primarily along the BamD TPR 3 and TPR 4 and along POTRA5 α1- β1 regions of BamA, and the L1 and L2 loop regions connecting them, resulting in 650 $Å^2$ of buried surface area.

Validation of crystal structure

While Rhodothermus BAM was useful for crystallization, expressing thermophilic proteins to use for the biochemical analysis would be difficult. Instead, a BamA-BamD structure from E. coli was generated from the Rhodothermus BamA-BamD structure. The E. coli interface is seen in figure 4. The two residues, BamA E373 and BamD R197, previously thought to be important in mediating the BamA-BamD interaction are seen in the binding interface, separated by approximately 1.5 Å. This supports that a salt bridge is likely forming and provides some initial validation of the model. Another likely interaction between BamA and BamD is between BamA R353 and BamD E178, which are approximately 2.0 Å. Several residues BamD are highly conserved across different diderm bacteria and occur in the predicted interface such as BamD R197, BamD Y177 and BamD A193 (Sandoval et al., 2011). Since maintaining the interface between BamA and BamD has shown to be essential for cell survival, it is encouraging that residues within the interface are conserved across species.

While the structure was consistent with previous biochemical data, it was important to directly verify that the solved BamA-BamD interface was physiologically relevant and not a byproduct of the fusion strategy. To validate the interface, the crystal structure was used as a guide to predict specific residues which would selectively disrupt the interface when mutated. The E. coli BamA-BamD interface was used as a model to make mutations, allowing the well characterized E. coli model system to be used for further biochemical validation.

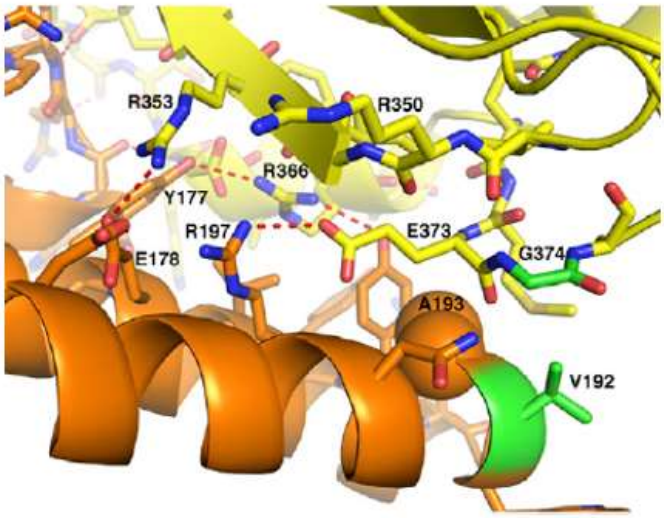

Figure 4. Interface of BamA-BamD from E. coli Crystal structure using E. coli Bam proteins were generated using the Rhodothermus model and the predicted interface for E. coli subunits is shown. Residue A193 is tightly packed in interface and is a target for tryptophan mutation. BamA E373 and BamD R197 are in close proximity consistent with previous studies. Possible coulomb interaction between BamA R353 and BamD E178, as well as highly conserved BamD Y177 directly in interface Green residues were targets for cysteine mutations for cross linking experiments briefly described.

To validate the solved interface, several residues where chosen to disrupt the BamA-BamD interaction. As discussed, BamA E373 and BamD R197 previously identified by Ricci et al., 2012 and predicted to interact were at the interface which gave initial support that the interface was correct. The experiments carried out by Ricci et al., 2012 were repeated to verify these residues were essential for BamA-BamD interaction. Furthermore, the small, conserved residue alanine A193 shown in figure 4 was mutated to a bulky tryptophan residue. The tryptophan residue was predicated to disrupt the interface from steric effects.

To determine if the two subunits interacted, complementation assays and pull down assays were used to. Because both BamA and BamD are essential proteins in the cell, the special cell lines were used for complementation assays and pull downs. E.coli BAM depletion strains JCM 166 and JCM 290 developed by Wu et al.,2005 were used . E. coli strain JCM166 contains the BamA gene under the control of arabinose promoter. In the presence of arabinose, BamA is expressed and the cells can grow. If cells are grown in glucose rich media, the promoter is repressed and endogenous BamA is depleted from cells after several generations leading to cell death. It was previously shown that a low copy plasmid expressing a N-terminal His-tag BamA can complement the BamA depletion strain, effectively replacing endogenous BamA with His-tagged BamA (Kim et al., 2007). By using the JCM 166 cell type along with the plasmid

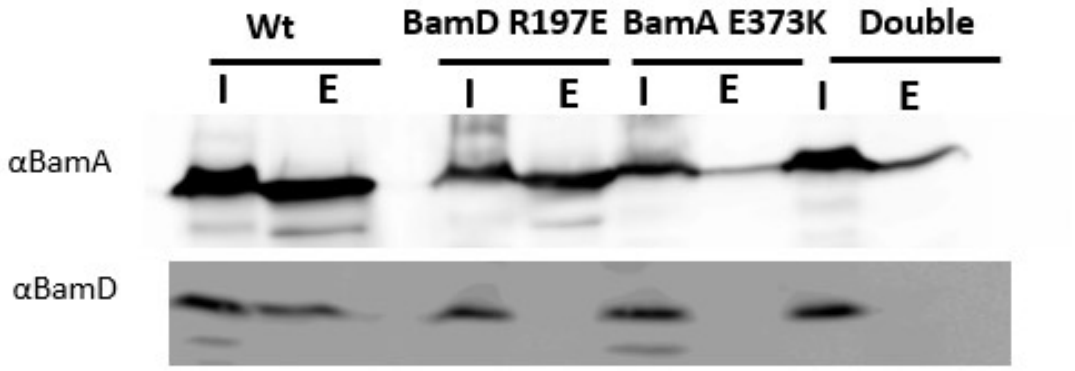

Figure 5. BamA-D interface validation with BamA E373K and BamD R197E
Effects of BamA E373K and BamD R197E on interface. Western Blot of input (I) and elution (E) Ni-NTA column pull down of His-tagged BamA from BamD depletion cells. BamD R197E does not copurify with wild type BamA and BamA E373K does not copurify with wild type BamD. Double mutant (BamA E373K/ BamD R197E) does not restore binding to detectable level.

containing tagged BamA, only BamA containing the His-tag would be present in the cell. JCM 290 cells have BamD under the same arabinose promoter allowing for depletion of endogenous BamD. The JCM290 and JCM 166 strains was used for both complementation assays and pull down assays as described below to deplete endogenous BamD or BamA respectively.

The lethal BamA E373K mutation and compensatory BamD R197E mutation previously identified by Ricci et al., 2012 are in close contact in the model. The two residues occur on the predicted interface and are separated by approximately 1.5 Å, suggesting they likely interact. It was confirmed that BamA E373K does not complement when transformed into the BamA depletion strain. The His tagged BamA E373K mutant was transformed into BamD depletion cells, so any BamD detected was from the plasmid copy. After purifying the mutant BamA, BamD failed to co-purify indicating the interface was disrupted (figure 5). The compensatory mutation on BamD R197E was also made. This BamD mutant could complement however it did

not co-purify with wild type BamA. This suggests that the BamD R197E mutant has a strong enough contact with BamA to remain functional but is too weak to pull down.

From the crystal structure, these two residues likely form a salt bridge. By mutating either residue to have the opposite charge, the interaction is weakened beyond detectable limits. If making one mutation causes coulombic repulsion, it is logical that making both mutations would recover the charge interaction. When this double mutant (BamA E373K/BamD R197E) was made, it was found to complement in both BamA and BamD depletion cells. However, when the mutant BamA is pulled down, the BamD mutant did not co-purify. The crystal structure indicates other charged residues at the BamA-BamD interface like BamA R350, BamA R353, BamA R366, and BamD E178 (figure 4). Therefore, a possible explanation why binding is not completely restored could repulsion from the other charged residues within the interface.

The small residue alanine (A193) on BamD sits in the interface in a tightly packed region. The alanine residue was mutated to a bulky tryptophan residue to attempt to disrupt the BamA-BamD interaction through steric hindrance. To test this hypothesis, a complementation assay with first done. The low copy plasmid pZS21 containing a N-terminal His tagged BamA and either wildtype or A193W BamD were transformed into the BamD depletion strain. Cells were grown overnight in arabinose and switched to glucose rich media. After several generations, the A193W mutant died while the wildtype continued to grow, indicating that the A193W BamD mutant failed to complement (data not shown). This suggested that the BamA-BamD interaction had been sufficiently weakened to disrupt enzymatic activity.

To confirm that the mutation was disrupting the interface, BamA was purified to see if BamD would copurify. If the interaction had been disrupted, BamD would not purify when BamA was pulled down. BamA depletions cells were transformed with a plasmid containing the

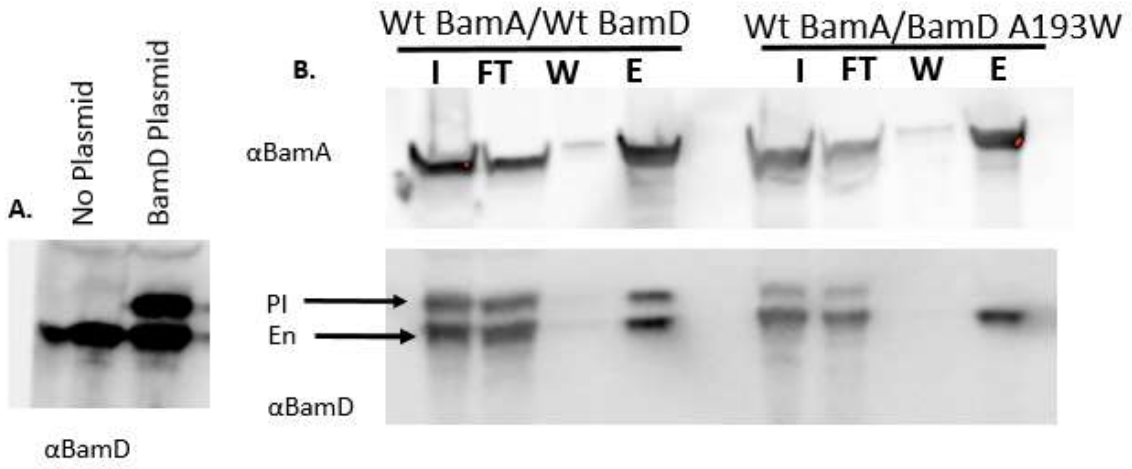

Figure 6. BamA-D interface validation with BamD A193W

A. 2.1 kDaTag on plasmid encoded BamD allows for discrimination between endogenous and plasmid BamD copies on gradient gel. Cells with no plasmid compared with cells transformed with tagged BamD and blotted against BamD.

B. Effect of BamDA193W mutations. Western blot from Nickel–NTA purification with column samples input (I), flow through (FT), column wash (W) and elution (E). Blotted with anti BamA (αBamA) and anti BamD (αBamD). His-tagged BamA is able to pull down both endogenous BamD (En) and plasmid encoded (PI) wild type BamD. BamD A193W mutant fails to co purify with BamA and is not present in elution.

His-BamA and the BamD A193W. BamA depletions cells were used so BamD could only interact with His tagged BamA and give a stronger signal in the pull downs. Since cells required endogenous BamD to grow, a tag was added to the plasmid BamD giving a 2.1 kDa weight difference. This allowed differentiation on an SDS-PAGE gel between endogenous and plasmid introduced copies of BamD (figure 6A). After endogenous BamA was depleted, cells were lysed and run over a Ni-NTA column. The samples were run on an SDS-gel and western blotted. In the control gel, there are two bands in the anti-BamD blot, which correspond to the endogenous (lower) and plasmid (upper) copies. Both these copies are present in the elution from the column, meaning that BamA could pull down endogenous and plasmid encoded copies of wild type BamD. However, when A193W BamD mutant was used, the interaction is lost. The plasmid encoded copy is present in the input of the column but is not in the elution. This indicates the mutant BamD did not bind with BamA and supports that the tryptophan mutation disrupted the interface beyond detectable limits.

The model was further supported through crosslinking experiments performed by Alex Hopkins in the Sousa Lab. Cysteines were engineered at two residues on the BamA-BamD interface highlighted in green in figure 4 with the correct orientation for disulfide bond formation. When the cysteine mutants were expressed, a cross-linked product was detected by both BamA and BamD antibodies. The cross-linking experiments further validates the model found.

From the protein pull downs, we were confident that the correct interface between BamA and BamD had been captured. Using the structure of the interface, the BamA-BamD interaction was selectively disrupted by putting a bulky tryptophan directly in the predicted interface. Interface disruption resulted in non-complementation and BamA and BamD no longer co purified. The solved interface was consistent with previous biochemical studies on the BamA and BamD interaction. Specifically, the importance of BamA E373 and BamD R197 in maintaining the BamA-BamD interaction is explained through the close charge interaction of the two residues.

The crystal structure of BamA-BamD along with the previously solved BAM fragments allows us to build a model for BamABCD. The full BamA structure from Neisseria with both the transmembrane domain and periplasmic POTRA domains (Noinaj et al., 2013) was used as a base. The POTRA domains from the BamA BamB fusion protein (Jansen et al., 2015) along with the POTRA 4-5 domains of the BamA-BamD fusion presented here were superimposed on the BamA backbone. The BamC BamD structure previously solved (Kim et al., 2011) was also superimposed on the BamA-BamD fusion structure. The resulting superposition provides a snapshot of a complete BAM complex, with only BamE and the C-terminal domain of BamC missing.

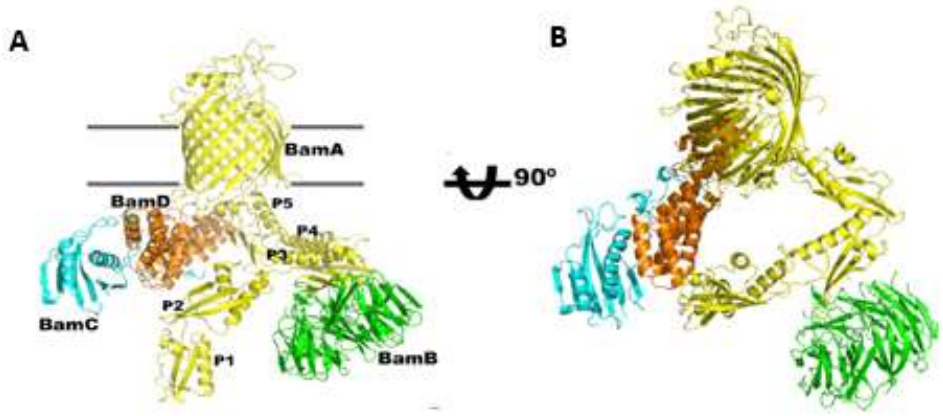

Figure 7. Model of E. coli BamABCD complex

A. Front view of BamABCD model built using previously solved structures along with BamA-BamD structure presented here. BamA (yellow) has β-barrel domain in membrane with POTRA 2-5 domains extending into the periplasm in a ring like fashion with BamD (orange). BamB (green) binds to POTRA3 and BamC (light blue) binds to BamD.
B. Top down view of BAM complex. View of BamD POTRA ring is parallel to the membrane which could be used to funnel and sequester OMPs before insertion in the membrane. Ring is approximately 30 Å by 60 Å

The model for BamABCD complex is shown in figure 7, with BamA shown in yellow, BamB in green, BamD in orange and BamC in blue. BamD along with the POTRA domains 2-5 form elliptical ring in the periplasm with the ring plane parallel to the membrane. Furthermore, POTRA 2 extends around and could have a possible contact point with BamD, however this interaction has not been experimentally proven. BamD also has potential contact points with the loop region between strands β6 and β7 of the β barrel transmembrane domain of BamA. These other potential contact points from the model represent a limitation of only crystallizing smaller fragments at a time. However, POTRA5 remains the largest and most essential contact between BamA and BamD.

The BamD-POTRA2-5 ring could represent a possible mechanism by which OMPs in the periplasm are funneled toward the membrane. A recent mechanism proposed and supported with cross linking experiments by lee et al., 2016 has an unfolded OMP binding to the POTRA

domains at one terminus and BamD at the other terminus. This binding of the termi restricts movement of the OMP and allows for β-hairpins to form. Binding of the OMP to BamD and POTRA5 would allow β-hairpin formation inside the POTRA2-5 ring seen in our model. The OMP would be kept close to the membrane and could be released through the lateral gating of BamA upon folding. While this hypothesis represents only one possibility, this model of BamABCD can be used to begin making mechanistic predictions about BAM mediated folding.

In vitro reconstitution of OMP folding

With a structural model of BAM, we can begin to probe the mechanism by which OMPs are folded and inserted into the outer membrane. However, since BAM is an essential component for bacteria growth, any in vivo testing that significantly disrupts the OMP folding pathway results in cell death. Having an in vitro assay which can fold β-barrels would allow more direct testing of the BAM mechanism. An in vitro model with BAM catalyzed OMP folding has already been developed (Hagan et al., 2010; Roman-Hernandez et al.,2014). The BAM complex is purified and reconstituted into liposomes. OMPs are purified separately and stabilized in urea. SurA, a periplasmic chaperone, is also added and is hypothesized to stabilize unfolded OMP in solution (Hagan et al, 2011). In this pre-purified OMP model, OMPs, SurA, and reconstituted BAM complex are combined and OMP fold into liposomes is observed.

While this system is useful, it relies heavily on a concentrated sample of outer membrane protein in a high concentration of urea to keep the OMPs denatured and prevent aggregation. The goal was to improve upon this model by more accurately capturing in vivo concentrations and conditions of proteins. Synthesizing proteins and immediately folding them would eliminate the need for urea. Protein synthesis would use an in vitro transcription/translation (**IVT**) system and would rely on the previously developed BAM/liposome reconstitution system.

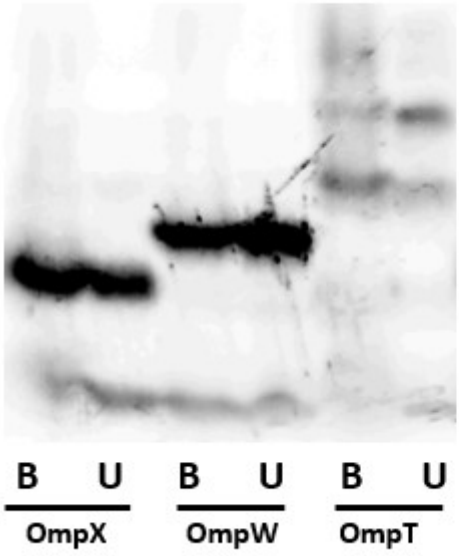

Figure 8. Expression of membrane proteins with in vitro transcription/translation
OmpX (20 kDa), OmpW (25 kDa), and OmpT (35 kDa) expressed in 0.15% Triton x-100. Boiled (B) and unboiled (U) samples run for each protein. OmpT band shift between boiled and unboiled could be possible folding but was not investigated further.

Two different in vitro transcription/translation systems were initially tested for protein expression. An E. coli extract based system was initially tested however low yields of the soluble protein control were initially obtained. Furthermore, since it is an extract from bacteria, it contains non-essential components like proteases which could interfere with the in vitro reconstitution of the OMP folding. Subsequently, the NEBPure system, reconstituted from purified E. coli components, gave stronger expression levels of a soluble control protein (data not shown). Since the NEBPure system is from purified components, it is less likely that components in the system will interfere with OMP folding. Therefore, the NEBPure system was chosen for use with the in vitro folding model.

The high background of the in vitro translation system made it difficult to visualize synthesized products on SDS-PAGE gels. Therefore, S^{35} methionine was added into the IVT reactions so synthesized protein would be radio labeled. Gels are vacuum dried and exposed to a phosphor screen before imaging with a Typhoon to detect radiolabeled protein.

While soluble proteins were easily expressed with the invitro transcription/translation system, membrane proteins are generally more difficult to express. Therefore, protein expression

of several different membrane proteins was tested with the IVT. The three outer membrane proteins OmpX, OmpW, and OmpT were initially tested for expression. As shown in figure 8, all three successfully expressed with the system into low levels of detergent (figure 8). OmpX was selected for further testing because it was relatively small, contained eight methionines for labeling, and had already been used previously for the other in vitro folding assays in the lab. OmpX is an eight stranded β-Barrel with a molecular weight of 20 kDa and is involved in bacterial adhesion (Voqt and Schulz, 1999).

Even though the OMPs expressed well, it was important to demonstrate that in vitro synthesized protein was capable of folding. To do this, conditions which favor OMP folding were used. It has previously been showed that urea-denatured OMPs will spontaneously fold into liposomes at an intrinsic folding rate without any BAM present. This intrinsic folding rate is dependent on the lipid composition (Surrey and Jahnig 1995). In liposomes made with native E. coli lipids, which are primarily phosphatidylethanolamines (PE) and phosphatidylglycerols (PG) (Gidden et al., 2009), the intrinsic folding rate is very slow which is why BAM is required to catalyze folding. However, by using liposomes made from phosphatidylcholine (PC) lipids, the intrinsic folding is high enough were significant OMP folding without BAM is observed. The intrinsic folding rate is also dependent on number carbons in the acyl chain, with shorter tail lengths associated with higher intrinsic folding rate (Gessmann et al., 2014). Since the initially we were only interested in the folding competence of vitro synthesized protein, liposomes made from PC lipids with short acyl chains (10 carbons) were used due to their high spontaneous insertion rates. This allowed expression and folding conditions to be optimized independently of reconstituted BAM system.

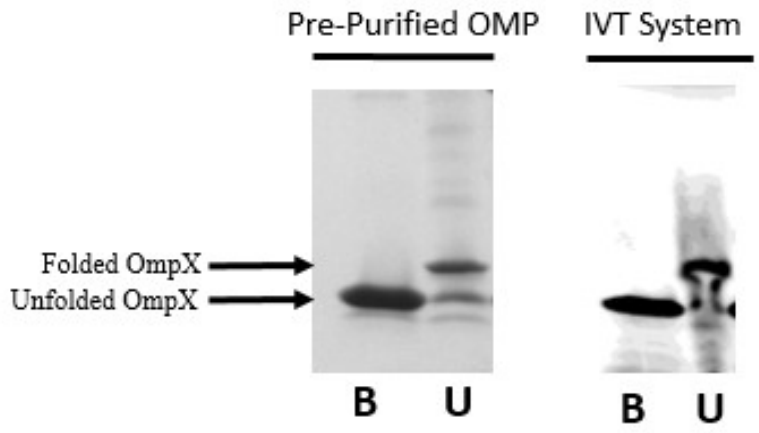

Figure 9. Heat modifiability assay of OmpX with sonication dispersed liposomes
Pre-purified OmpX combined with sonication dispersed liposomes run on SDS-PAGE gel after incubation and coomassie stained (left). Presence of higher band in unboiled (U) compared with boiled (B) indicates folded OmpX. In vitro synthesized OmpX with sonication dispersed liposomes and S^{35} on gel transferred to phosphor screen and imaged. Similar Band shift between boiled and unboiled again indicates folding.

Liposomes were made by resuspending lipid films in buffer with detergent and dispersing with sonication. Lipids were diluted with buffer to lower the concentration of detergent below the critical micelle concentration to induce liposome formation and collected through ultracentrifugation. Folding was then determined through a heat modifiability assay. Since β-barrels are stable in SDS when unboiled and the folded form will run at a different weight on an SDS-PAGE gel. Folding can be assessed through the differential mobility of a boiled and unboiled sample on a SDS, with OmpX running at a higher weight when it is folded.

To test for folding competency of IVT protein, liposomes composed of PC lipids, which favor spontaneous folding, were added to the in vitro system. S-35 methionine was added to label any synthesized product along with the periplasmic chaperone SurA which is hypothesized to prevent aggregation. The pre-purified OMP system was run in parallel as a folding control for

the heat modifiability assay. The samples from both trials were run on an SDS PAGE gel to see if folding occurred.

IVT synthesized protein was shown to be folding competent. The pre-purifed system with urea denatured OmpX was used as a control for OMP folding. As seen in figure 9, the weight shift between boiled and unboiled samples illustrates folded OmpX. A similar weight shifted band is observed in the unboiled lane in figure 9 corresponding to IVT folded OmpX. This illustrates that IVT OMPs are physically able to fold. Folding experiments were repeated several times however folding was not observed in every reaction. This suggests that the IVT system is sensitive and conditions can be further optimized. Another consideration was that there were low levels of residual detergent in the liposome preparation. Since OMPs fold efficiently in detergent, the folded band could be OmpX folded in detergent or a mixed micelle rather than liposomes. This could also explain why folding was observed sporadically, as the detergent levels between liposomes preps could vary. Further experiments with liposomes made in the absence of detergent is necessary to eliminate this possibility.

Overall, a proof of concept for a new in vitro OMP folding system based on an in vitro transcription translation system with liposomes has been presented. IVT was shown to successfully synthesize outer membrane proteins. While inconsistent, IVT proteins were also shown be folding competent through a heat modifiability assays. Several steps need to be taken before direct BAM activity can be ascertained with this in vitro system. First, folding in the complete absence of any detergent should be demonstrated. Next, the system would need to be recombined with reconstituted BAM complex. While procedures exist for reconstituting the BAM complex, it will likely require optimization to get catalytically active BAM working with the IVT system. The IVT requires specific salt and buffer concentrations for protein synthesis,

which could prove in compatible with the BAM complex. However, if the reconstituted BAM could fold IVT protein, it would represent a significant improvement in replicating the in vivo folding pathway compared to the current urea dependent in vitro model currently used.

Materials and Methods

Purification for Crystallization

Fusion constructs were cloned into modified pHD plasmid obtained from Dr. Wang (Institute of Biological Chemistry, Academia Sinica, Taipei, Taiwan). A 6x Histidine tag and small ubiquitin-like modifier (SUMO) at the N-terminus of the target gene to facilitate expression, purification, and tag cleavage. Plasmids 1066 (BamA POTRA1-5 BamD), 1150 (BamA POTRA3-5 BamD), and 1151 (BamA POTRA4-5 BamD) were transformed in BL21(DE3) cells and plated on LB Kanamycin plates. A single colony from the plate was used to start a 10 ml overnight culture of LB/Kan. This was used to inoculate 6 L of LB/Kan which were grown at 37ºC to an OD_{600} of 0.6. The cultures were cold shocked in an ice bath for 1 hour. BamA-BamD fusion protein expression was induced with 0.4 Mm Isopropyl β-D-1-thiogalactopyranoside (IPTG) and grown at 20 ºC overnight. Cells were spun down and resuspended in buffer A (25 mM Tris pH 8.0, 150 mM NaCl), protease inhibitor cocktail tablet (Roche), and Benzonase (Novagen) before being homogenized (EmulsiFlex C3). Cell lysate was spun down at 31,000 x g for 30 minutes. Soluble lysate was loaded onto Ni-NTA column equilibrated with buffer A and let incubate for 1 hour at 4 ºC. The column was washed with 5 column volumes of buffer A followed by 5 column volumes of buffer B (25 mM Tris pH 8.0, 150 mM NaCl, 20 mM imidazole). Protein was eluted in 3 column volumes of buffer E (25 mM Tris pH 8.0, 150 mM NaCl, 200 mM imidazole). Pms 1151 (BamA POTRA4-5 BamD) was soluble and purified well. The His-tag was cleaved with a ULP-1 protease and with 1 mM 2-mercaptoethanol overnight. Protein was then run through size exclusion chromatography

(Superdex 200 Amersham Pharmacia Biotech). Fractions were collected, concentrated to 12 mg/mL and stored at -80 ºC with 1mM TCEP.

Protein crystallization and data collection

Crystallization screening of BamA (POTRA 4-5) BamD fusion protein was carried out at 16 oC with sitting drop vapor diffusion method. Hampton Research (HR) crystal screen and crystal screen 2, along with HR PEG/LiCl, HR Membfac, Wizard crystal screens 1 and 2, and Molecular Dimensions Morpheus screen. Crystallizing conditions were refined with hanging drop in 10% PEG-3000, 15% 2-Propanol and 0.1M HEPES pH 5.6, combining 1.5 µL of mother liquor and 1.5 µL of 12 mg/mL protein at 25 oC. Crystals formed after a week and thin plates. Crystals were harvested and cryoprotected in mother liquor supplementedwith 20% Ethylene Glycol before being flash frozen in liquid nitrogen at 100K. An X-ray diffraction dataset was collected at the Advanced Light Source of the Lawrence Berkeley National Laboratory and solved using molecular replacement. Rhodothermus structure was then projected onto E. coli BamA and BamD to generate E. coli structure.

Copurification and Western Blots

E. coli strain JCM 166 and plasmid pZS21 were a gift from Dr. Thomas Silhavy (Princeton University) (Wu et al., 2005). His-tagged BamA and BamD with a 2.1 kb tag were cloned into pZS21 to make the wild-type control. The following mutations were made: BamD R197E, BamD A193W, BamA E373K and BamA E373K/BamD R197E. JCM 166 (BamA depletion cells) or JCM 290 (BamD depletion cells) were transformed with plasmid and plated on LB/Kan 0.1% arabinose plates. A single culture was used to inoculate 5ml overnight culture of LB/Kan 0.1% arabinose at 37ºC. Cells spun down and washed twice in fresh LB and used to

inoculate a 5ml culture of LB/Kan 0.1% glucose. Cells were grown at 37ºC to OD_{600}~0.6 and diluted down to OD_{600} of 0.05 to keep cells in log phase. This was repeated four times until negative control strain died due to Bam depletion. The final 5 ml culture was used to inoculate a 200 mL culture of LB/Kan 0.1% glucose. This was grown to OD_{600} of 0.6 and spun down in 100 mL aliquots. Cell weight was determined and solubilized in 5 ml Bugbuster™/gram of cells (~1.5mL) along with Halt™ Protease & Phosphatase Inhibitor cocktail (Thermo Scientific), 100ug/mL lysozyme, and 2 µL Benzonase (Novagen). Cells were resuspended in lysis buffer and incubated for 1 hr with rocking at room temperature. Cell lysate was spun down for 20 minutes at 21,000 x g and pH was brought up to 8.0. Soluble lysate was added on to 500 µL Ni-NTA 50% slurry (Qiagen) which was pre-equilibrated with buffer D (10 mM Tris pH 8.0, 150 mM NaCl, 0.5% Triton-X100) and incubated at room temperature for 45 minutes with periodic agitation. Ni-NTA column was washed with 5 column volumes of buffer D and eluted in 100 µL fractions of buffer E (buffer D and 500 mM Imidazole). The second elution fraction, along with the last 250 µL wash fraction, and input were mixed with SDS loading dye, boiled for 5 minutes, and run on 4-20% (GenScript) SDS-PAGE. Gels were transferred to PVDF membranes (EMD Millipore) and probed with BamA (1:20,000) or BamD (1:5,000) polyclonal Antibodies raised against these proteins (Cocalico Biologicals, Inc.) and secondary stained with Goat Anti-Rabbit HRP conjugate (Pierce) (1:25,000) Western Lightning ECL Pro HRP substrate (PerkinElmer) were used for detection.

Sonication Liposome Prep

Lipid films were made from Avanti Polar Lipids 10:0 PC lipids. Lipid films stored at -20 ºC were brought to 25 ºC and resuspended in 200 ul of 50 mM Tris, 150 mM NaCl pH 8 +0.03% DDM to give final lipid concentration of 20mg/ml. Suspension was lightly vortexed for 30

seconds and let settle for 5 minutes six times. Suspension was sonicated at 25 ºC for two hours to disperse lipids. Lipid suspension were diluted into 8 mL of 200 ul of 50 mM Tris, 150 mM NaCl and incubated for 45 minutes. Lipids were further diluted to 39 ml and ultra-centrifuged (Beckman L8-70M, Ti 70 fixed angle rotor) at 54,500 rpm for 2 hours. Buffer was decanted and pellet was washed and resuspended in 200 ul of 50 mM Tris pH 8 and stored at 4 ºC used within one week.

In vitro Expression

NEB PURExpress In Vitro Protein Synthesis Kit was used for all protein expression. Following manufactures instructions, 7.5 ul of solution B (Ribosomes, T7 Polymerase, tRNAs) was added to 10 ul of Solution A (Amino acids, NTPs, Phospocreatine). SurA (final concentration of 10 µL), S-35 Methinone (Perkin Elmer) at 0.6 µL, 10 µL of liposomes (final concentration ~2.5 mg/ml) and water were combined for a final volume of 30 µL. Reaction was initiated by adding 200 ng of target DNA and incubating with shaking 37 ºC for 2-3 hours.

Pre-purified OmpX controls

OmpX was overexpressed in BL21 cells and purified in inclusion bodies. Protein was run over anion exchange column and eluted in 8 M urea, concentrated and stored at -80 ºC. Aliquots were thawed on ice. In a separate tube, 10 ul of liposomes (final concentration ~3.5 mg/ml), SurA (final concentration 10 µL), and 50 mM Tris buffer pH 8 were combined for a final volume of 27.5. OmpX is added to give a total volume of 30 µL, giving a final OmpX concentration of 3 µL and 0.66 M urea. Samples incubated with shaking 37 ºC for 2-3 hours.

Gel Folding Assay

Reactions were cooled on ice for 20 minutes and SDS loading dye was added. Reactions were split into equal volumes and one aliquot from each reaction was boiled at 95 ºC for 5 minutes. Reactions were loaded onto 4-20% gradient gels (Biorad Mini-ProteanTGX). Running buffer was cooled down to 4 ºC. Gels were run at 150V. Gels were cut to separate in vitro translated product and pre-purified lanes. Pre-purified lanes were stained in coomassie and imaged. In vitro translated protein lanes were dried between filter paper (Whatman) and plastic wrap in a vaccum at 80 ºC for one hour. Dried gel was placed in phosphor plate casseset overnight and imaged using Typhoon imager.

Acknowledgments

First, I would like to thank my research adviser Professor Marcelo Sousa for his invaluable support and advice throughout the project, as well as Alex Hopkins for his help with the structure validation and general guidance. I would like to express my gratitude to Sandra Metzner helped immensely with cloning of all the constructs used for the project as well as Dave McKay for his assistance in the crystallography core. I would also like to thank Arden Doerner and Marc-Andre LeBlanc in the Sousa lab who provided helpful advice with the in vitro folding as well as general assistance. Finally, I would also like to thank my committee members Professor Joseph Falke and Professor Jennifer Martin.

References

Albrecht, R., and Zeth, K. (2011). Structural basis of outer membrane protein biogenesis in bacteria. J. Biol. Chem. 286, 27792–27803.

Endo, T., Kawano, S., and Yamano, K. (2011). BamE structure: the assembly of beta-barrel proteins in the outer membranes of bacteria and mitochondria. EMBO Rep. 12, 94–95.

Gessmann, D., Chung, Y. H., Danoff, E. J., Plummer, A. M., Sandlin, C. W., Zaccai, N. R., and Fleming, K. G. (2014) Outer membrane beta-barrel protein folding is physically controlled by periplasmic lipid head groups and BamA, Proc. Natl. Acad. Sci. USA 111, 5878-5883.

Gatzeva-Topalova, P.Z., Walton, T.A., and Sousa, M.C. (2008). Crystal structure of YaeT: conformational flexibility and substrate recognition. Structure 16, 1873–1881.

Gatzeva-Topalova, P.Z., Warner, L.R., Pardi, A., and Sousa, M.C. (2010) Structure and flexibility of the complete periplasmic domain of BamA: the protein insertion machine of the outer membrane. Structure 18: 1492–1501.

Gidden, J., Denson, J., Liyanage, R., Ivey D., Lay, J. (2009) Lipid Compositions in Escherichia coli and Bacillus subtilis During Growth as Determined by MALDI-TOF and TOF/TOF Mass Spectrometry. Int J Mass Spectrom. 283(1-3): 178-184

Hagan, C.L., Kim, S., and Kahne, D. (2010). Reconstitution of outer membrane protein assembly from purified components. Science 328, 890–892.

Hagan, C.L., Silhavy, T.J., and Kahne, D. (2011). Beta-Barrel membrane protein assembly by the Bam complex. Annu. Rev. Biochem. 80, 189–210.

Jansen, K.B., Baker, S.L., and Sousa, M.C. (2015). Crystal structure of BamB bound to a periplasmic domain fragment of BamA, the central component of the beta-barrel assembly machine. J. Biol. Chem. 290, 2126–2136.

Kim, S., Malinverni, J.C., Sliz, P., Silhavy, T.J., Harrison, S.C., and Kahne, D. (2007). Structure and function of an essential component of the outer membrane protein assembly machine. Science 317, 961–964.

Kim, K.H., and Paetzel, M. (2011). Crystal structure of Escherichia coli BamB, a lipoprotein component of the beta-barrel assembly machinery complex. J. Mol. Biol. 406, 667–678.

Kim, K.H., Aulakh, S., and Paetzel, M. (2011). Crystal structure of beta-barrel assembly machinery BamCD protein complex. J. Biol. Chem. 286, 39116–39121.

Knowles, T.J., Browning, D.F., Jeeves, M., Maderbocus, R., Rajesh, S., Sridhar, P., Manoli, E., Emery, D., Sommer, U., Spencer, A., et al. (2011). Structure and function of BamE within the outer membrane and the beta-barrel assembly machine. EMBO Rep. 12, 123–128.

Koebnik, R., Locher, K. P. and Van Gelder, P. (2000), Structure and function of bacterial outer membrane proteins: barrels in a nutshell. Molecular Microbiology, 37: 239–253.

Lee J. et al. (2016). Characterization of a stalled complex on the β-barrel assembly machine. Proc. Natl. Acad. Sci. USA 113, 8717–8722.

Lyu, Z.X., and Zhao, X.S. (2015). Periplasmic quality control in biogenesis of outer membrane proteins. Biochem. Soc. Trans. 43, 133–138.

Malinverni JC,Werner J, Kim S, Sklar JG, Kahne D, et al. 2006. YfiO stabilizes the YaeT complex and is essential for outer membrane protein assembly in Escherichia coli. Mol. Microbiol. 61:151–64

McPherson, A., Cudney, B. (2014) Optimization of crystallization conditions for biological macromolecules. Acta Crystallogr F Struct Biol Commun. 70(Pt 11): 1445–1467

Nakamura, K., and Mizushima, S. (1976) Effects of heating in dodecyl sulfate solution on the conformation and electrophoretic mobility of isolated major outer membrane proteins from Escherichia coli K-12, J Biochem 80, 1411-1422.

Nikaido,H. (2003). Molecular basis of bacterial outer membrane permeability revisited Microbiol. Mol. Biol. Rev., 67 (2003), pp. 593–656

Noniaj, N., Rollauer, S., Buchanan., S. (2015) The β-barrel membrane protein insertase machinery from Gram-negative bacteria. Curr Opinion in Structural Biolgoy. 31, 35-42.

Onufryk C, Crouch ML, Fang FC, Gross CA. 2005. Characterization of six lipoproteins in the σE regulon. J. Bacteriol. 187:4552–61

Patel, G. J., and Kleinschmidt, J. H. (2013) The lipid bilayer-inserted membrane protein BamA of Escherichia coli facilitates insertion and folding of outer membrane protein A from its complex with Skp, Biochemistry 52, 3974-3986.

Plummer, A. M., and Fleming, K. G. (2016) From Chaperones to the Membrane with a BAM!, *Trends Biochem. Sci. 41*, 872-882.

Ricci, D.P., Hagan, C.L., Kahne, D., and Silhavy, T.J. (2012). Activation of the Escherichia coli beta-barrel assembly machine (Bam) is required for essential components to interact properly with substrate. Proc. Natl. Acad. Sci. USA 109, 3487–3491.

Roman-Hernandez, G., Peterson, J. H., and Bernstein, H. D. (2014). Reconstitution of bacterial autotransporter assembly using purified components. *eLife* **3**, e04234

Sandoval, C.M., Baker, S.L., Jansen, K., Metzner, S.I., and Sousa, M.C. (2011). Crystal structure of BamD: an essential component of the b-Barrel assembly machinery of gram-negative bacteria. J. Mol. Biol. 409, 348–357.

Santiago, J., Guzman, G.R., Torruellas, K., Rojas, L.V., and Lasalde-Dominicci, J.A. (2004). Tryptophan scanning mutagenesis in the TM3 domain of the Torpedo californica acetylcholine receptor beta subunit reveals an alpha-helical structure. Biochemistry 43, 10064–10070.

Sklar, J.G., Wu, T., Kahne, D., and Silhavy, T.J. (2007b). Defining the roles of the periplasmic chaperones SurA, Skp, and DegP in Escherichia coli. GenesDev. 21, 2473–2484. Sutcliffe, I.C. (2010). A phylum level perspective on bacterial cell envelope architecture. Trends Microbiol. 18, 464–470.

Silhavy TJ, Kahne D, Walker S. The bacterial cell envelope. Cold. Spring Harb. Perspect. Biol. 2010;2(5):a000414

Surrey, T., and Jahnig, F. (1995) Kinetics of folding and membrane insertion of a beta-barrel membrane protein, *J. Biol. Chem. 270*, 28199-28203.

Voqt, J., Schulz, GE. (1999). The structure of the outer membrane protein OmpX from Escherichia coli reveals possible mechanisms of virulence. Structure 7(10):1301-9

Warner, L.R., Varga, K., Lange, O.F., Baker, S.L., Baker, D., Sousa, M.C., and Pardi, A. (2011). Structure of the BamC two-domain protein obtained by Rosetta with a limited NMR data set. J. Mol. Biol. 411, 83–95.

Wolfram, Z. (2014). Secretion of Bacterial Lipoproteins: Through the Cytoplasmic Membrane, the Periplasm and Beyond. Biochim Biophys Acta. 2014 August ; 1843(8): 1509–1516.

Wu, T., Malinverni, J., Ruiz, N., Kim, S., Silhavy, T.J., and Kahne, D. (2005).Identification of a multicomponent complex required for outer membrane biogenesis in Escherichia coli. Cell 121, 235–245.